MDPI

Article

Calibrating Microscopic Traffic Simulation Model Using Connected Vehicle Data and Genetic Algorithm

Abolfazl Afshari, Joyoung Lee *, Dejan Besenski, Branislav Dimitrijevic and Lazar Spasovic

John A. Reif, Jr. Department of Civil & Environmental Engineering, New Jersey Institute of Technology, Newark, NJ 07102, USA; abolfazl.afshari@njit.edu (A.A.); besenski@njit.edu (D.B.); dimitrijevic@njit.edu (B.D.); lazar.spasovic@njit.edu (L.S.)
* Correspondence: jo.y.lee@njit.edu; Tel.: +1-973-596-2475

Abstract: This study introduces a data-driven approach to calibrate microscopic traffic simulation models like VISSIM using high-resolution trajectory data, aiming to improve simulation accuracy and fidelity. The study focuses on a highway segment of NJ-3 and NJ-495 in Hudson County, New Jersey, selected as a case study for its high traffic volume and strategic significance. Trajectory data from 338 connected vehicles, sourced from the Wejo dataset, a global provider of anonymized, high-resolution vehicle movement data, along with traffic volume data from Remote Traffic Microwave Sensors (RTMS), served as inputs. The trajectories produced by the simulation model were compared to the ground truth to measure discrepancies. By adjusting driving behavior parameters (e.g., car-following and lane-changing behaviors) and other factors (e.g., desire speed), a Genetic Algorithm was adopted to minimize these differences. Results showed significant improvements, including a 14.19% reduction in mean error, an 18.27% reduction in median error, and a 22.57% reduction in the 75th percentile error during calibration. In the validation phase, the calibrated parameters yielded a 32.68% reduction in mean error, demonstrating the framework's robustness. This study presents a scalable calibration framework using connected vehicle data, providing tools for accurate simulation, real-time traffic management, and infrastructure planning.

Keywords: traffic microsimulation models; calibration; connected vehicles; trajectories; driving behavior parameters; Genetic Algorithm; VISSIM

1. Introduction

Traffic simulation models are essential to traffic management and urban planning, as they provide information on traffic patterns and the possible effects of infrastructure modifications without requiring actual trials. These models have been utilized for years in traffic management and have gained even greater importance with the recent development of transportation networks. In such environments, the ability of simulation models to closely mimic real-world traffic becomes crucial. Several studies have shown how well traffic simulation models mimic actual conditions and maximize traffic flow in both urban and highway environments [1]. However, traffic simulations can also have limitations, such as high computational demands and reliance on accurate calibration for reliable results. By ensuring that traffic simulation models accurately represent actual conditions, accurate calibration makes it possible to evaluate transportation policy, infrastructure investments, and traffic management tactics. Simulation results might differ greatly from real traffic behavior if they are not calibrated properly, which reduces their usefulness in decision-making.

Numerous parameters must be calibrated in traffic microsimulation software to fine-tune traffic and driver behaviors. However, identifying optimal values for these parameters is a complex task. Additionally, traffic engineering simulations are usually confined to specific areas to save time and costs, even though the designated areas are sometimes influenced by external traffic. For instance, congestion on a highway may cause backups in downstream traffic, which is miles away. In such cases, simply expanding the simulation's spatial coverage may not always be the solution.

The necessity to solve issues by calibrating traffic simulation models in scenarios with significant traffic variations and connected vehicle data served as the motivation for this research. Conventional methods for calibrating traffic simulation models often rely on giving predetermined parameter values or simple numerical ranges for particular driving behaviors or network configurations. Although these methods are straightforward, they are not adaptable enough to take into consideration the particularities of different networks, such as geometry, traffic patterns, and driver behavior. When used in a variety of real-world scenarios, this may result in inadequate calibration outcomes. A one-size-fits-all strategy is unlikely to produce the required degree of precision in various scenarios since the value of each calibration parameter is fundamentally dependent on the particular network design and driving behavior characteristics. In order to overcome these constraints, this paper presents a novel calibration framework that adapts parameter changes to the particular circumstances of the network being represented. This method allows traffic simulation models to be calibrated particularly for the target network. Although this study demonstrates the suggested framework on a particular highway segment, it is intended to be flexible and applicable to any network. Because of this, it is a flexible and reliable tool for improving the accuracy of traffic simulation models in a variety of applications, beyond the constraints of preset parameter values, and enabling context-sensitive optimization.

To increase the accuracy of microscopic traffic simulation models like VISSIM, this study presents a calibration framework that combines high-resolution connected vehicle trajectory data with traditional traffic volume data. As VISSIM is a popular tool in traffic engineering and offers a stable platform for simulating sophisticated traffic systems, it was selected for this investigation. Furthermore, automated and iterative optimization is made possible by its adaptable Component Object Model (COM) interface, which is essential for the suggested methodology. In the current study, a microsimulation model was created for a highway segment calibrated as a case study to test the framework. During the calibration process, vehicle trajectory data from the Wejo dataset, a comprehensive collection of connected vehicle data, were utilized alongside Remote Traffic Microwave Sensor (RTMS) data to create a traffic volume dataset used as an input in the simulation model. Using the two mentioned datasets, vehicles in the simulation were divided into two groups: connected vehicles from the Wejo dataset and non-connected vehicles from the RTMS dataset. The trajectory data from connected vehicles were essential for the remainder of the study. After the simulation period, these trajectories were extracted and compared to real-world traffic trajectories to identify discrepancies. In subsequent iterations, driving behavior parameters were adjusted to make the trajectories more similar. By employing a Genetic Algorithm (GA) and repeating this process, the differences between the trajectories were minimized, and optimal values for driving behavior parameters were determined.

The absence of high-resolution data, the difficulty of parameter adjustments, and the computational burden of iterative simulations are some of the major issues in traffic simulation calibration that are addressed in this study. The work maintains computational efficiency while achieving notable reductions in calibration errors through the use of GA and

distributed computing. The findings show how including cutting-edge data sources, such as connected vehicle trajectories, can improve traffic models' precision and dependability, making them a more effective tool for traffic management and infrastructure development. The study's findings show promise for greatly increasing the accuracy of traffic simulations, which directly affects advanced traffic management and infrastructure design.

The primary objective of this research is to improve the fidelity of microsimulation models by creating a novel calibration framework that makes use of traffic volume measurements and connected vehicle trajectory data. The study aimed to improve model fidelity by minimizing the differences between simulated and real vehicle trajectories using a GA. This section provides a brief introduction to the study. After a quick review of the literature, the specifics of the suggested methodology are presented in the next section. The outcomes of this study are thoroughly explored in the results and discussion sections, which are presented last.

2. Literature Review

In the field of traffic engineering, the fidelity of simulation models is paramount for predicting and enhancing real-world traffic scenarios. Calibration methodologies have evolved significantly [2], yet the integration of high-resolution data from connected vehicles represents a promising frontier that has yet to be fully exploited. This literature review explores the advances and challenges in the calibration of microscopic traffic simulations, underscoring the potential for dramatically improved accuracy and applicability. These models require accurate adjustments of parameters to reflect real-world conditions. Because of the complexity of these models and the variety of traffic situations and locations, it is not easy to find an optimum solution to calibrate the models. While researchers have made lots of efforts and studies to find a fast, accurate, and inexpensive solution [3], still, none of them can be generalized to all traffic and environmental situations. These studies vary from traditional techniques to advanced algorithms [4,5], from small road segments [6] to large-scale traffic networks [7], and each has its advantages and challenges. Popular microsimulation software like SUMO and AIMSUN have been used for similar investigations because of their resilience and flexibility. However, VISSIM was selected for this study due to its compliance with automated optimization via the Component Object Model (COM) interface and its capacity to integrate data from connected vehicles.

Despite various calibration approaches presented in the literature, a key challenge remains, which is integrating high-resolution, connected vehicle data to improve model accuracy across diverse traffic networks. Recent studies introduced various methods for calibrating traffic models. Leal et al. [8] aimed to calibrate the AIMSUN simulator for a network in Brazil by utilizing a GA to minimize the mean absolute error of the delay time between the simulation and observed data, which were vehicle speed and volume measurement captured in different intersections of the networks. The results showed a significant improvement compared to the default values of parameters in the model. They did not, however, evaluate how well the recommended methods worked in practice. In a study conducted by Arafat et al. [9], VISSIM simulation software was calibrated for intersections in Miami, Florida, specifically regarding the degree of saturation. The data collected during the green times, along with queue lengths, were then compared with the real-world data. There were some limitations such as a small sample size and specific intersection geometry design, which can be considered for expanding the calibration applicability.

The Bayesian methods for calibrating traffic models were tested in some studies [10–12]. The application of Bayesian neural networks with heuristic algorithms to predict simulation results without actually running simulations was tested recently [13]. This approach cap-

tured the optimal parameter values without repeated simulation runs. Physics-informed machine learning has been used to enhance the calibration process and results in some studies [5,14]. They used a physics-informed machine-learning approach [5] and deep reinforcement learning [14] to calibrate the model. Keane and Gao [4] used the adjoint method to minimize the root mean square error between the simulations and measurements. Some recent studies considered a data-driven calibration approach. By continuously recording data from loop sensors inside the network, Hwang et al. [15] dynamically optimized the origin–destination matrix in microscopic traffic simulation. However, the availability and quality of the data heavily affect the performance of this method.

While high-resolution data in the calibration of traffic simulators play a pivotal role, capturing accurate data may not be straightforward [16]. Langer et al. [17] aimed to calibrate the Simulation of Urban Mobility (SUMO) to create a testing environment for automated driving systems. They captured high-resolution trajectory data using devices installed in the vehicles driving through the network. A GA was used to find the best solution and minimize the error between simulated and observed data. Samandar et al. [18] integrated drone capabilities to collect high-resolution data in a roundabout. In a similar study, Hale et al. [19] used drones and helicopters to capture vehicle trajectories and used them to calibrate the traffic models. Both studies were able to calibrate the traffic model using collected data continuously, yet the duration of data collection in the suggested approaches was limited.

Practical implementation of the suggested methods demonstrates their performance in improving the traffic model calibration. In a study conducted by Chaudhari et al. [6] in India, data collected by cameras during a short period in a segment of roadway without any intersection or interruption with pedestrians were used to calibrate the Wiedemann 99 car-following model, one of the most used models in traffic engineering. The study showed significant improvement in the model, although there is a need to test the same approach in a more complex network. Additionally, the Wiedemann 99 car-following model was calibrated for bicycle traffic by Kaths et al. [20]. This study compared data captured from a bicycle simulator to the results obtained from the VISSIM traffic simulation. The calibrated parameters performed better than the default ones, although capturing the wide range of behaviors was unsuccessful. Some studies tried to calibrate the simulation model in specific situations such as work zones [21,22], roads with limited sight distance [23], and exact locations with a particular traffic behavior [24]. Table 1 compares some of the recent efforts to calibrate microsimulation models and provides details about them.

Some challenges of calibrating microsimulation models still need to be solved despite significant progress. Issues such as improving the accuracy of the models, generalized solutions, and fast and reliable methods need to be considered. In this study, the high-resolution trajectory of vehicles inside the network was used to process the calibration. This approach helps to obtain the best possible accurate results compared to past studies. Because of its shown effectiveness in resolving complicated optimization problems and its capacity to efficiently explore vast solution spaces, the GA was selected. Its advantage over conventional techniques in calibrating traffic models was shown in earlier studies [8,17,25], which makes it a reliable tool for parameter adjustment in a variety of circumstances. Moreover, the nature of the proposed platform makes it suitable for all types of networks with every type of traffic and environment.

Table 1. The literature review on the calibration of microsimulation models.

Author	Simulation Software	Calibration Method	Data Used	Key Results
Figueiredo et al. [26]	AIMSUN (version 7.0.4)	Sensitivity analysis of calibration parameters	Simulated data with introduced errors in calibration parameters	Established relationships between calibration parameter errors and simulation output accuracy; highlighted the importance of parameters like reaction time and minimum distance between vehicles
Otković et al. [27]	VISSIM *	Neural network-based calibration focusing on travel time prediction	Field data from roundabouts in an urban area	Showed that neural network predictions can effectively calibrate microsimulation models, improving accuracy in travel time and queue parameter estimations
Mauro et al. [28]	AIMSUN *	Hypothesis testing to match speed–density relationships	Traffic data from the A22 Brenner Freeway, Italy	Achieved a good match between simulated and observed speed–density relationships, validating the calibration approach
Hale et al. [19]	VISSIM *	Genetic Algorithm	Vehicle trajectories and volumes	Achieved high fidelity between simulation and real-world data for multi-lane highway systems
Chun et al. [23]	SIDRA, TransModeler *	Gap acceptance parameters	Video-based trajectory data	Calibration improved travel time and delay accuracy for sight-restricted roundabouts
Zhao et al. [22]	VISSIM *	Iterative adjustment (VisVAP)	Vehicle speeds and travel times	Calibrated for real-time adaptive queue detection; validated travel speed reductions
Gao et al. [29]	VISSIM *	Multi-point distribution calibration optimization method	NGSIM trajectory data	Improved calibration accuracy by about 9% using multi-point distribution calibration; combining global and local parameter calibration yielded results more consistent with actual driving characteristics
Abdeen et al. [24]	VISSIM *	GEH statistic	Traffic volumes, travel speeds, travel time	Calibration focused on local driver behavior parameters; improved simulation accuracy
Haque et al. [21]	VISSIM *	Statistical inference (empirical distributions)	Travel times, saturation headways	Demonstrated spatial transferability of calibrated parameters for Nebraska work zones

* Version not specified.

3. Methods

This section presents the study's methodology in detail. This study's primary objective is to provide a methodical calibration procedure that will bring a simulation model closer to actual traffic behavior. In the first subsection, the overall designed architecture of the system is presented. Then, the data preparation process is explained in detail, followed by the calibration parameters. In the simulation process subsection, the details about the simulation setup and execution are described. Subsequent subsections provide insights into the optimization and evaluation strategies used to refine the model's accuracy, ensuring that the simulated results align closely with real-world data. Using connected vehicle data and traffic flow measurements, the methodology offers a thorough understanding of how the simulation calibration is carried out, optimized, and validated.

3.1. Overall Architecture

The process presented in this study consists of multiple stages. The overall process is summarized in Figure 1. A server handles the main process and controls other resources and computers. In the current study, an Intel NUC 12 Pro Mini PC running the Ubuntu 20.04.5 LTS operating system is used. However, due to the nature of the code, any computer with any operating system can perform the server function. As the ground truth, the trajectories of connected vehicles must be obtained. To create the simulation model, vehicle volume should be collected from the real world. If the connected vehicle dataset contains information about all the vehicles in the network, it can be used to calculate vehicle volumes for the simulation model. In most traffic networks, the market penetration of connected vehicles is not one hundred percent. Therefore, this study suggests using a traffic data collection method capable of counting vehicle volumes at multiple locations within the network. This dataset is useful for determining the total number of vehicles driving in the network, including connected and non-connected vehicles. The combination of these two datasets is used to create an origin–destination (O/D) matrix, which serves as the input for the VISSIM simulation network. The data from connected vehicles are used separately to evaluate the calibration process. Having the O/D matrix and vehicle trajectories, the server is ready to start the calibration process.
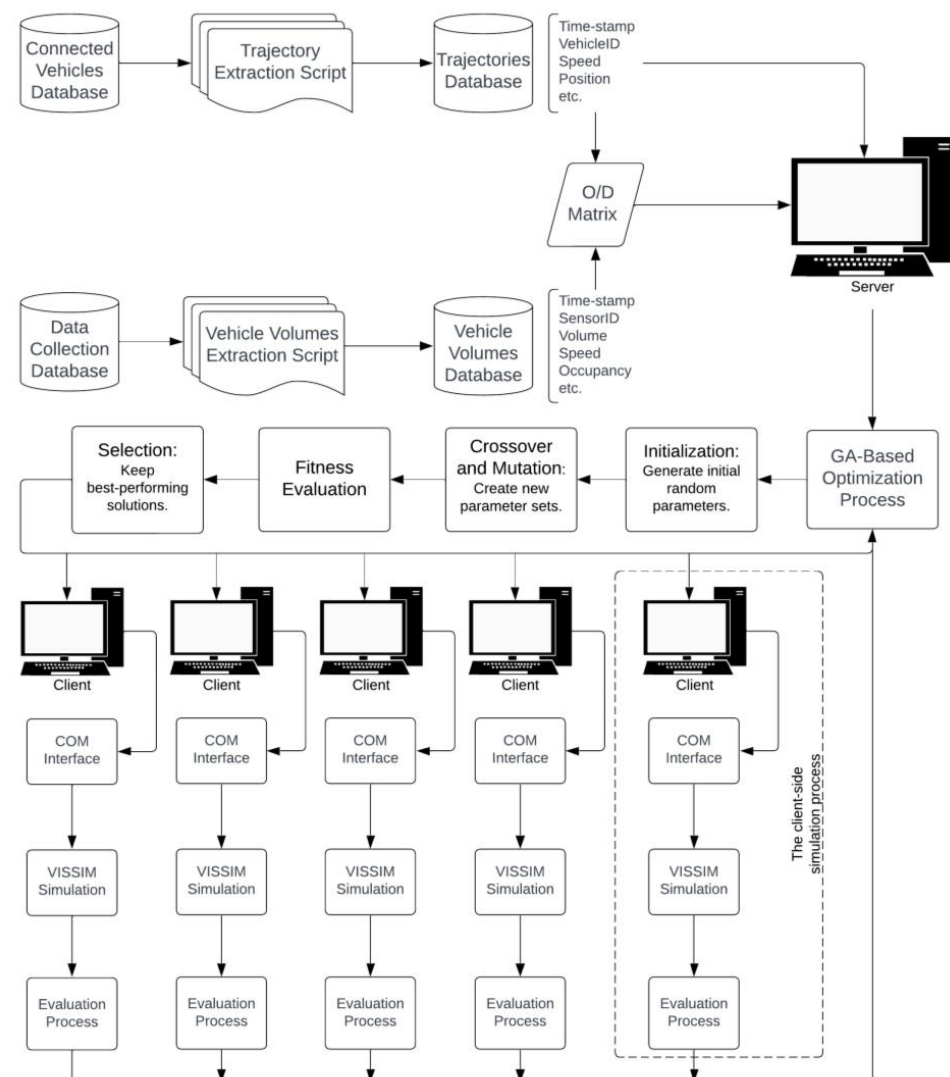

Figure 1. Overview of the proposed calibration framework, including server and client processes. The client-side simulation process is detailed in Figure 2.
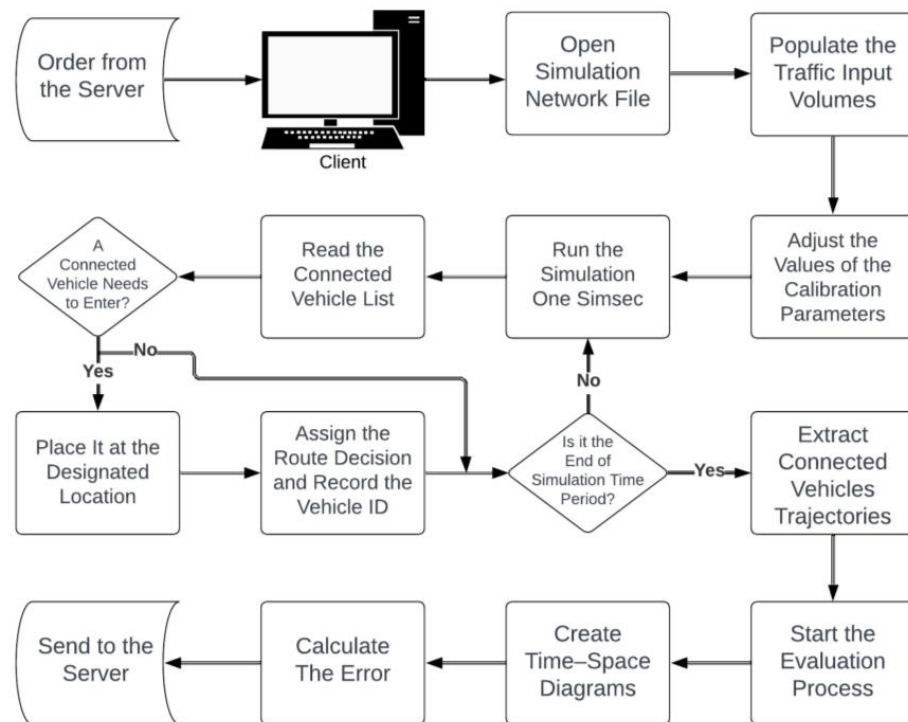
Figure 2. Detailed client-side process within the calibration framework, as referenced in Figure 1.

Calibrating a microscopic simulation model is a non-trivial task that generally demands numerous repetitive simulation runs with different parameter values. To expedite the process, instead of running the simulation on a single computer, this research adopts a distributed computing architecture, allowing multiple computers (i.e., clients) to conduct simulation tasks and send the results back to the server. Multiple desktop and laptop computers running the Windows 11 operating system are used as clients in this study. The clients utilize the Component Object Model (COM) interface to control the VISSIM software Version 2024.00-10 (PTV Group, Karlsruhe, Germany) which is discussed briefly in the following subsections. The server generates multiple sets of values for calibration parameters and sends these sets, along with the O/D matrices and vehicle trajectories, to the clients one by one. Each client uses the O/D matrix as input for the VISSIM model and automatically changes the default values of calibration parameters according to the server's instructions. After running the simulation, the results are compared to the vehicle trajectories, which serve as the ground truth. Each client evaluates the current calibration process and sends the results back to the server. The server then gathers all the results and attempts to optimize the calibration parameters for the next iteration. More details about these stages are presented in the following subsections.

3.2. Data Preparation

As mentioned above, the presented architecture requires two datasets as input for the VISSIM simulation model: the O/D matrix, which contains all types of vehicle origins and destinations within the network, and connected vehicles' trajectory data. To create the O/D matrix, a traffic detection method should be applied within the network. The number of vehicles moving through the network should be countable using this way. If the connected vehicle dataset achieves one hundred percent market penetration, there is no need to use any other data collection method. However, such a comprehensive dataset is currently unavailable in most traffic networks. In this study, RTMS are used to collect historical traffic volume data (passenger car equivalent) within the network. Installing multiple sensors at

various locations within the network facilitates the creation of an O/D matrix easily using simple calculations. Both the Wejo dataset and RTMS dataset are available upon request.

The connected vehicles' trajectories are extracted from the Wejo dataset. The Wejo dataset is a collection of connected vehicle data that captures detailed trajectories and behavioral information of vehicles on real-world roads. In this dataset, each vehicle is assigned a unique Journey Identification (JID). For each JID, information, such as longitude and latitude, speed, and time-stamps, is recorded every second. The Wejo dataset must first be filtered for the road network under consideration because it includes data on connected vehicles traveling all roads. Using the geofencing method, all vehicles outside the designated network are filtered out. In the geofencing method, some polygons around the area of interest are defined. Any GPS coordinates outside of these polygons are excluded from the dataset. By completing this process, the noise in the data is reduced, and only relevant trajectories are included. Moreover, the dataset needs to be filtered for the specific project period.

Having cleaned the dataset, a script is designed to prepare the datasets for input into the VISSIM simulation model. This script first examines all connected vehicle trajectories within the network during the simulation period to capture vehicle origins, destinations, and entry times into the network. It then creates a list of this information, making it ready for the main script to place the vehicles in the simulation at the exact times and locations corresponding to the real world and assigns route decisions to the vehicles based on their destinations. All the vehicles created in the simulation using this method are categorized as connected vehicles. Meanwhile, all the vehicles created in the simulation using the O/D matrix derived from the RTMS data are categorized as non-connected vehicles. To refine the data, all vehicles from the Wejo dataset are subtracted from the RTMS dataset based on their time-stamps and locations.

3.3. Calibration Parameters

For calibration, this study selects multiple parameters within VISSIM software (version 2024), primarily from the "driving behavior" section of the freeway menu. The Wiedemann 99 model, recommended for freeways and incorporating ten parameters, is chosen as the "car-following model". Historical data from some highways indicate that traffic flow is influenced by external conditions such as upstream congestion, and merging and diverging outside of the network. To account for these factors alongside driving behavior parameters, a dummy highway link, featuring one exit and one entrance along with a reduced speed area to simulate congestion, should be attached to the end of the highway segment. The trajectories of vehicles on this dummy link are not considered in the calibration process. In addition to driving behavior parameters, the calibration process allows for adjustments to the number of vehicles entering, the dimensions and speed of the reduced speed area, and the relative flow of cars using the exit on the dummy link. Table 2 shows all the parameters that can be adjusted in VISSIM software (version 2024) for calibration purposes in this study.

Table 2. Parameters in the calibration process.

Short Name	Long Name	Description	Unit	Default	Min	Max
LookAheadDistMax	Lookahead distance (maximum)	A vehicle's maximum forward vision allows it to respond to other vehicles ahead or to its side (inside the same link).	m	250	100	400
AccDecelOwn	Accepted deceleration	The lower limit of the vehicle's lane changes deceleration.	m/s^2	−1	−10	0

Table 2. *Cont.*

Short Name	Long Name	Description	Unit	Default	Min	Max
CoopDecel	Maximum cooperative deceleration	Cooperative braking during maximum deceleration.	m/s^2	−3	−10	0
LookBackDistMax	Look back distance (maximum)	The farthest a car can see behind it to respond to other cars behind it (inside the same link).	m	150	50	250
MaxDecelOwn	Maximum deceleration	Maximum lane-changing deceleration according to the designated routes for the overtaking vehicle.	m/s^2	−4	−10	−0.01
NumInteractObj	Number of interaction objects	Within its maximum lookahead distance, the smallest number of downstream cars and relevant network objects (signal heads, limited speed zones, etc.) to which a vehicle responds.	-	2	1	10
NumInteractVeh	Number of interaction vehicles	The maximum number of cars downstream to which a vehicle can respond. Other network objects are not included in this.	-	99	1	99
SafDistFactLnChg	Safety distance reduction factor (lane change)	(1) The trailing vehicle's safety distance on the new lane, which is used to decide whether to perform a lane change; (2) the lane changer's safety distance; and (3) the distance to the slower, preceding lane changer.	-	0.6	0	1
W99cc0 *	Standstill distance	The ideal spacing between two cars at a stop.	m	1.5	0.5	1.5
W99cc1 *	Gap time distribution	In addition to the standstill distance, a driver's desired gap time in seconds, which is calculated from the time distribution.	s	0.9	0.5	30
W99cc2 *	'Following' distance oscillation	The maximum distance that a driver following another car will consciously go beyond the preferred safety distance before purposefully approaching.	m	4	0	15
W99cc3 *	Threshold for entering 'BrakeBX'	At the beginning of the deceleration process, the time in seconds until the vehicle reaches the upper limit of the following distance to a slower leading vehicle.	s	−8	−30	0
W99cc4 *	Negative speed difference	The threshold for the relative speed during the subsequent process as compared to a slower leading vehicle.	m/s	−0.35	−1	0
W99cc5 *	Positive speed difference	The threshold for the relative speed during the subsequent process when compared to a quicker leading vehicle.	m/s	0.35	0	1
W99cc6 *	Distance dependency of oscillation	Distance's impact on relative speed thresholds during the subsequent procedure.	Rad/s	11.44	0	25
W99cc7 *	Oscillation acceleration	Minimal rate of acceleration or deceleration during the subsequent oscillation process.	m/s^2	0.25	0	1
W99cc8 *	Acceleration from standstill	Acceleration when beginning at a complete stop.	m/s^2	3.5	1	8

Table 2. *Cont.*

Short Name	Long Name	Description	Unit	Default	Min	Max
W99cc9 *	Acceleration at 80 km/h	80 km/h acceleration.	m/s^2	1.5	0.5	3
LenRedSpeed	Length of reduced speed area	The length of the reduced speed area in the dummy links at the end of the network.	m	-	0	888
DSRedSpeed	Desire speed in reduced speed area	Desire speed in reduced speed area.	km/h	-	5	70
VolInterFlow	Volume of interrupting flow	The number of vehicles that merge into the dummy link to interrupt the main flow.	vehicle/h	-	0	2000
RelFlowExit	Relative flow of exit at the dummy link	The percentage of vehicles that exit the network at the dummy link.	%	-	0	0.5
LnChgDist	Lane change distance before connectors	The distance before the connector where cars whose routes or paths cross it attempt to select the lane that will get them there without changing lanes.	m	200	100	2000
DesSpeed	Desire speed	Desire speed of vehicles in the network.	km/h	90	70	120

* Wiedemann 99 parameter.

3.4. Simulation Process

To run the simulation, each client receives an order from the server. This order includes a simulation run ID, the O/D matrices, the list of connected vehicle information, and values for calibration parameters. The client then opens the VISSIM simulation network, which has already been created and saved in the directory, and starts controlling it using the COM interface. The COM interface of VISSIM is a powerful mechanism that allows programmatic control of VISSIM. This interface is a tool for conducting automated and complex simulation tasks that need high levels of customization and dynamic data handling. The automated process in this study is conducted by multiple Python codes, which were able to interact with VISSIM using the COM interface.

The client uses the received O/D matrix to populate the traffic input volumes in VISSIM software (version 2024), which, based on the available data from RTMS, can be set at 5 min intervals. Consequently, multiple O/D matrices are entered into the software, one for every five min. The client then starts to adjust the values of the calibration parameters based on the received order. The client runs the simulation for one Simsec, equivalent to 0.1 s. Meanwhile, the client checks the connected vehicle dataset and places the connected vehicle at the designated location if it needs to enter the network at that moment. It also assigns the route decision to the vehicle and records the vehicle ID for future purposes. The client then simulates another step and repeats this process until the end of the simulation.

After the simulation ends, the client captures and saves the trajectories of the connected vehicles based on their IDs, which are ready to be compared with the ground truth. This comparison is necessary to evaluate the accuracy of the calibration parameters in this run. To ensure statistical robustness and to reduce bias, each client processes the order from the server five times with different random seeds and reports back the median values of the results. Figure 2 presents a summary of the simulation process for each client.

3.5. Optimization and Evaluation Processes

As presented in the previous subsection, the proposed calibration method requires an evaluation process and optimization. Making the simulation model as close to the ground truth as possible is the main goal of this process. This is accomplished by the process's design, which aims to align the connected vehicles' trajectories in the simulation with those in the real world. Furthermore, comparing these two trajectories is chosen as the main evaluation process in this study. A time–space diagram is created for each connected vehicle in the network to facilitate this comparison. Then, the trajectories from both the real world and the simulation are plotted on this diagram. The area between these two curves in the time–space diagram is defined as the error of the simulation results. Figure 3 illustrates a conceptual time–space diagram with two curves representing hypothetical trajectories from the real world and the simulation in red and green, respectively. The error for this vehicle can be calculated using Equation (1).

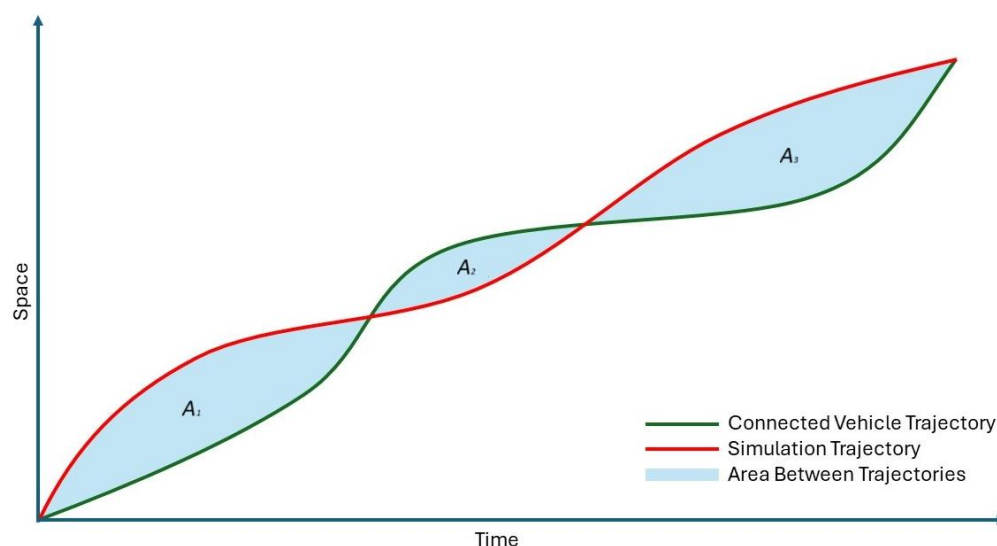$$Error = \sum A_i = \sum (|S_j - C_j|) \tag{1}$$

Figure 3. Conceptual time–space diagram.

In Equation (1), A_i represents the area between the two trajectory lines. The total error is considered as the simulation error for each vehicle. Each trajectory is divided into time intervals of 0.1 s to calculate this area. The value of space for the connected vehicle trajectory (C_j) is subtracted from the value of space for the simulation trajectory (S_j). The error is the summation of the absolute values of these differences for each time interval.

For every simulation run, the summation of errors for each vehicle represents the total error for that simulation. The optimization algorithm aims to minimize this total error. To optimize the calibration parameters in the VISSIM microsimulation model, a Genetic Algorithm (GA) is employed due to its effectiveness in handling complex optimization problems with multiple parameters and nonlinear relationships. By simultaneously examining several regions of the solution space, GAs conduct a global search, decreasing the possibility of becoming stuck in local minima [30]. Furthermore, the GA is appropriate for complex optimization situations when the objective function is neither convex nor differentiable since they do not require gradient information nor convexity assumptions. It can be efficiently parallelized, as each individual's fitness evaluation is independent. This aligns with the architecture, where multiple clients can run simulations concurrently, enhancing computational efficiency. Previous studies successfully applied GAs for calibrating traffic

simulation models, demonstrating their effectiveness in finding optimal or near-optimal solutions [8,25].

To reduce the differences between the simulated and actual vehicle trajectories, the GA iteratively changes the parameters in Table 2 within predetermined limits. The objective function of the GA is presented in Equation (2).

$$Minimize f(\theta) = \sum_{i=1}^{N} \sum_{t=1}^{T} |(S_{it}(\theta) - C_{it})| \tag{2}$$

In this equation, all of the calibration parameters used in the VISSIM simulation model are included in the parameter vector θ, which determines the goal function in this equation, $f(\theta)$. N is the number of vehicles, T_i is the number of time points for vehicle i, C_{it} is the observed coordinates of vehicle i at time t, and S_{it} is the simulated coordinates of vehicle i at time t as a function of the calibration parameters θ. The objective function aims to minimize the total simulation error by reducing the discrepancies between the simulated and real-world trajectories of connected vehicles. The function calculates the total error by summing the areas between the trajectory curves of each vehicle in the simulation and its corresponding real-world trajectory. These areas represent the differences in position over time between the simulated and real data; thus, a smaller area (and therefore a smaller sum of these areas) indicates a more accurate simulation. The GA optimizes the parameters of the simulation to achieve the lowest possible total error, improving the fidelity of the simulation model relative to the real-world conditions.

To ensure optimal performance of the GA, a systematic evaluation of its parameters—population size, mutation rate, number of generations, and crossover rate—is conducted, considering the trade-offs between computational efficiency and solution quality. To balance the algorithm's exploration and exploitation capabilities and guarantee convergence to an optimal or nearly optimal solution without incurring undue computing costs, these parameters must be carefully chosen. The population size determines how many potential solutions (sets of calibration parameters) are evaluated in each generation. A larger population provides a diverse set of solutions, enhancing the algorithm's ability to explore the search space but increasing computational load. A population size of 32 is chosen based on a trade-off between computational efficiency and solution quality. This size is sufficient to maintain genetic diversity without overwhelming computational resources [31]. In order to avoid stagnation at local optima, the mutation rate introduces new genetic material into the population by regulating the likelihood of random changes in the parameters of the individuals. A mutation rate of 0.1 is selected to provide a balanced introduction of variability. This rate is commonly used in GA applications and is effective in maintaining diversity within the population [32]. The crossover rate in the implemented GA is set at 100%, meaning crossover is applied in every reproduction step. This decision is based on the need to maximize exploration of the solution space by ensuring a consistent combination of genetic material from parent solutions. While a 100% crossover rate might not suit every problem, it is a common practice in GAs, particularly when paired with an effective mutation operator [32]. The mutation rate, set at 10%, complements the crossover process by maintaining genetic diversity and preventing premature convergence. This combination proves effective, as demonstrated by the algorithm's ability to improve fitness values and reduce calibration errors across generations iteratively. The number of generations defines how many iterations the GA will perform, influencing the depth of the search process. A total of 200 generations is deemed appropriate to allow the algorithm to converge toward an optimal solution while keeping computation time reasonable.

3.6. Site Description

As a case study, a section of NJ-3 and NJ-495 eastbound highways in Hudson County, New Jersey, is selected. This section is 2.75 km in length and connects Bergen County in New Jersey to Manhattan, New York City, New York, through the Lincoln Tunnel. As this road serves as one of the connections from the urban areas in New Jersey to the district areas in New York and also connects the Meadowlands Sports Complex (MetLife Stadium) to New York City, it is one of the most crowded roadways in the New York Metropolitan Area. The selected highway segment starts at milepost 9.2 on NJ-3 East and ends at milepost 0.95 on NJ-495 East. Figure 4 shows the selected segment on Google Maps. The highway in the selected segment has two exits to the local roads and other highways and one merging section from NJ-495, which are considered in the study. The first half of the section has three lanes, which are reduced to two lanes in the middle of the section after an exit to another highway. The section then becomes four lanes after a merge from NJ-495 in the last quarter of its length.
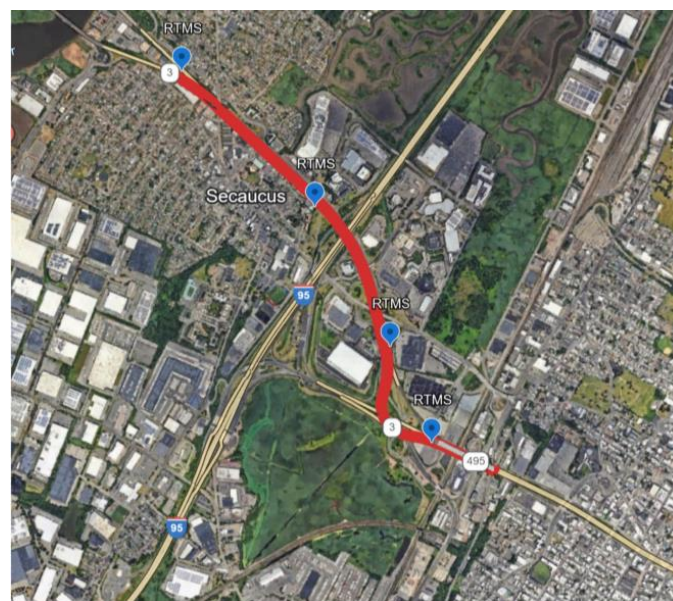

Figure 4. The selected highway segment (NJ-3 and NJ-495) on Google Maps alongside the locations of the RTMS.

The historical trajectory data for 7 July 2021, from 1 PM to 4 PM—which are the peak hours—are extracted from this dataset. The datasets provide sufficient traffic volume and vehicle trajectory data for the calibration process, though it is important to acknowledge that the data collection occurred during the COVID-19 period. By mid-2021, traffic volumes were rebounding; however, some effects of the pandemic may have persisted. Using geofencing methods, all trajectories outside the selected segment are filtered out. Overall, 338 individual connected vehicles passed through the highway section in the mentioned period. This trajectory dataset is then used as the ground truth in this study.

Four RTMS at multiple locations collect historical traffic volumes, enabling the counting of vehicles entering, driving through, and exiting the segment. Figure 4 shows the locations of these sensors on the highway segment. To refine the O/D matrix, the number of connected vehicles from the Wejo dataset is subtracted from the RTMS dataset. Finally, for every five min of the simulation, the O/D matrix for non-connected vehicles is created and incorporated into the simulation.

After each simulation run with predefined parameters, the script extracts the trajectories of vehicles to produce the time–space diagram for each vehicle and calculates the

error to be minimized during the calibration process, as explained in the previous sections. The VISSIM microsimulation model's parameters are optimized using a GA to improve its correspondence with ground truth data. The GA iteratively adjusts parameters in Table 2 within predefined ranges. At each iteration, the algorithm mutates these parameters with a set mutation rate to explore a variety of configurations. The fitness of each configuration is assessed based on how closely the simulated vehicle trajectories match the actual vehicle trajectories from the Wejo dataset. A population of possible solutions is created, their performance is assessed, and the top performers are chosen for the following generation.

The GA continuously adjusts driving behavior parameters to reduce the differences between the simulated and real-world data. In this study, 200 generations and 32 populations are conducted with a mutation rate equal to 0.1. These parameters are chosen based on their previous successful application in calibrating traffic simulation models such as [25] and available resources. By striking a balance between exploration and convergence, these values guarantee that the algorithm can successfully reduce the differences between simulated and actual trajectories.

4. Results

This section provides a summary of the study's findings. Although the general procedure and idea can be applied to any traffic network with any features, the study was carried out on a highway segment as a case study. This 2.75 km part of the NJ-3 and NJ-495 eastbound highways has three lanes in the first half, two lanes in the third quarter, and four lanes in the last quarter. It also has two exits to local roads and other highways as well as a section that merges from NJ-495. High traffic volumes and the significance of connecting urban regions to district areas led to the selection of this route. The selected segment, with moderate to high traffic, typical merging areas, and standard geometric features, represents a typical roadway environment, supporting the method's generalizability. However, unique geometric attributes or traffic characteristics in other sites may require minor adjustments to the calibration process.

4.1. Calibration Results

This study conducted 32,000 simulation runs to calibrate the network (200 generations, 32 populations per generation, and 5 runs per population). Each run used a warm-up period of 300 s and stopping criteria based on simulation duration. To account for variability, the five runs per population were conducted using different random seeds, which altered the arrival times and distribution of non-connected vehicles. However, for connected vehicles, the script consistently placed them at the same starting point and time to ensure consistency in their trajectories. All runs were performed under a single demand scenario, representing peak-hour traffic conditions, as described in Section 3.6. of the paper. It took around 616 h to complete the simulations, with each generation taking approximately 3 h. With nine clients on duty most of the time, each replication took approximately 5 min on average at the fastest possible speed. Figure 5 illustrates the results of the Genetic Algorithm. In this graph, the vertical axis represents the lowest median error of all populations for each generation. At each population, the median error across five simulation runs was calculated, and the best (lowest) error from all populations was selected as the representative result for that generation. The horizontal axis shows the generations of the GA. This graph indicates that the procedure found the optimal parameter settings and effectively reduced the discrepancies between the simulation trajectories and the actual world. Moreover, most of the reductions in errors occurred in the first quarter of the iterations, indicating that the process found the optimal solution faster than expected.
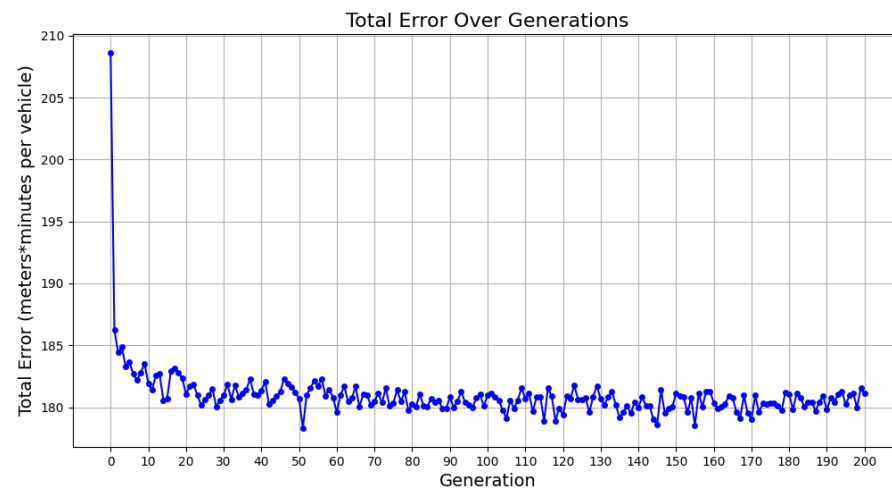
Figure 5. The results of the GA, showing the lowest median error across all populations for each generation.

Figure 6 shows time–space diagrams (TSDs) for three randomly selected vehicles out of the 338 connected vehicles in the dataset that can be matched with the Wejo trajectories. The selection was conducted randomly without bias to ensure typical results were represented. In these diagrams, vehicles are represented by lines, where steeper slopes correspond to slower speeds. The left-hand side TSDs illustrate the trajectory differences before the calibration process, while the right-hand side ones show the trajectory differences after the calibration process for the same vehicle. Improved alignment of the simulated vehicle trajectories with the ground truth trajectories, as seen in the right-hand side diagrams, demonstrates the effectiveness of the calibration process in making the simulation more representative of actual traffic behavior.

Table 3 details the total errors before and after the calibration process. Based on the provided statistical analysis, several insights emerge that highlight the effectiveness of the calibration process. Initially, the mean error decreased from 208.53 m·min to 178.94 m·min, reflecting a 14% decrease in mean error, indicating an improvement in overall accuracy. The median error, which represents the midpoint of error distribution, also saw a notable reduction from 131.56 to 107.53 m·min, indicating that at least half of the error values are now significantly lower and signify more consistent performance across different traffic conditions. The standard deviation, which measures the range of error values, went from 236.58 to 222.66, indicating that errors are more consistent after calibration. The minimum and maximum errors also improved, with the maximum error reducing from 2249.19 to 2170.08, which suggests a reduction in the most extreme cases of error.

Table 3. Statistical results of the errors in time–space diagrams before and after the calibration process.

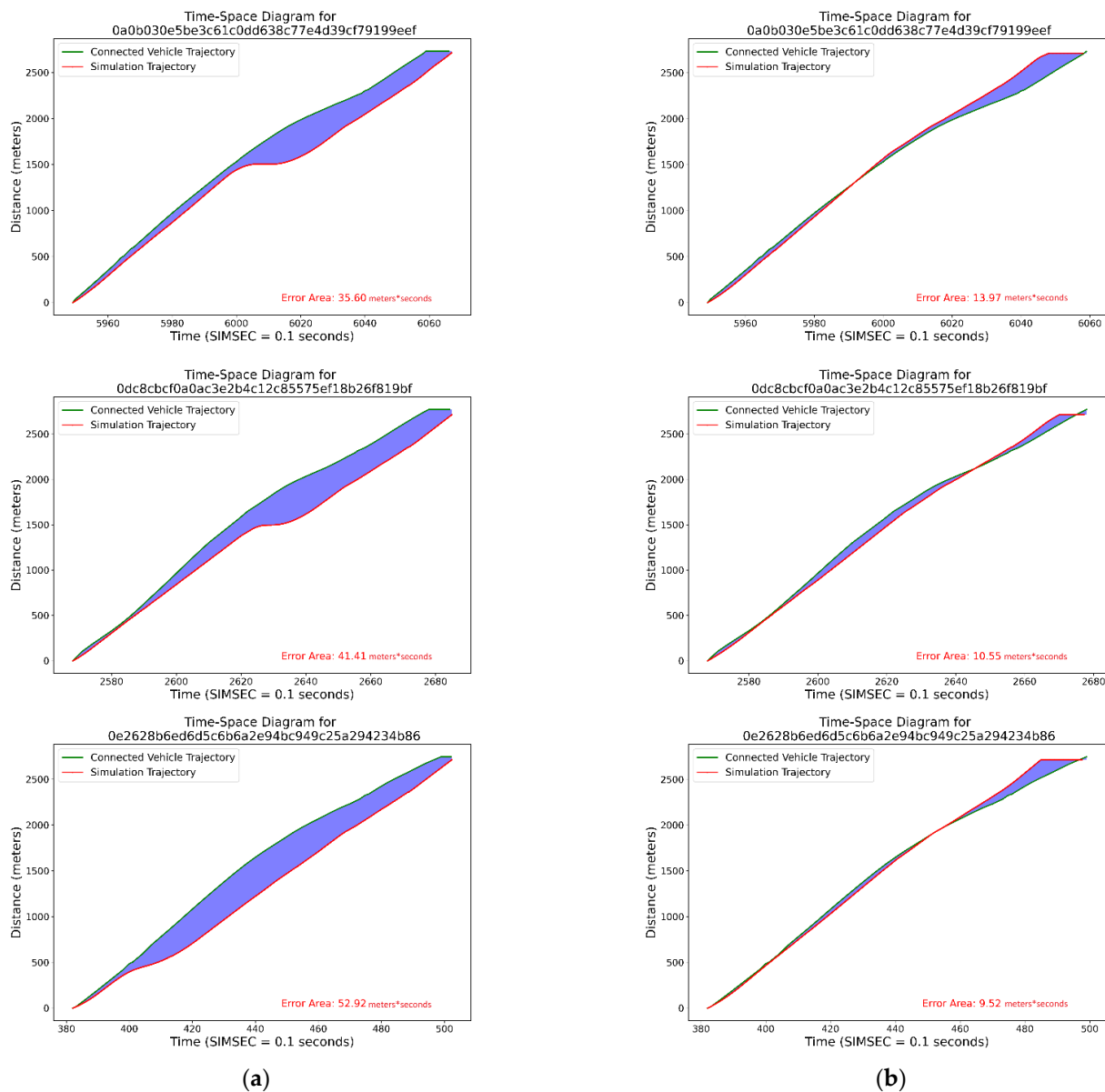| Errors in Time–Space Diagrams	Before Calibration	After Calibration	% of Change	Units
Mean	208.53	178.94	14.19%	m·min
Median	131.56	107.53	18.27%	m·min
Standard Deviation	236.58	222.66	5.88%	m·min
Minimum	3.14	1.66	47.14%	m·min
Maximum	2249.19	2170.08	3.52%	m·min
25th percentile	34.22	32.42	5.27%	m·min
75th percentile	310.90	240.73	22.57%	m·min
Variance	55,969.14	49,579.17	11.42%	$(m·min)^2$
Skewness	2.76	3.29	−19.25%	-
Kurtosis	16.27	19.93	−22.44%	-
Coefficient of Variation	1.13	1.24	−9.68%	-

Figure 6. Time–space diagrams before (**a**) and after (**b**) the calibration process, highlighting error reduction.

Percentile values give a deeper insight into the distribution of errors. The 25th percentile saw a slight improvement (5.27%), indicating that lower error values are becoming more common. More substantial is the improvement in the 75th percentile, decreasing from 310.90 to 240.73, showing that higher errors have been effectively reduced. Moreover, the variance decreased from 55,969.14 to 49,579.17, confirming a reduction in the spread of error data around the mean. Interestingly, the skewness and kurtosis increased from 2.76 to 3.29 and from 16.27 to 19.93, respectively, indicating that the distribution of errors has become more positively skewed and peaked post-calibration. A slight increase in variability, as indicated by kurtosis, points to remaining outlier cases that need further investigation. Lastly, the coefficient of variation increased from 1.13 to 1.24. This increase indicates a higher relative variability in error distribution relative to the mean after calibration, which suggests variability in the effectiveness of the calibration across different cases.

Overall, the alignment between the simulated and ground truth trajectories has improved, as evidenced by the decrease in the mean and median errors. These measures show the simulation model's overall accuracy as well as its primary tendency. The observed drop in the mean error can be attributed to the calibration's successful reduction in bigger

discrepancies, as indicated by the decrease in the 75th percentile error. This suggests that high-error instances were effectively handled by the calibration framework, resulting in a more realistic simulation. When compared to similar research [21,29], the method presented in this study performed better.

The increase in kurtosis and skewness indicates that although overall errors decreased, the distribution of errors became more positively skewed and peaked. This suggests that there are now fewer but more significant outliers and a greater percentage of errors are concentrated closer to the bottom end of the distribution. These outliers likely reflect specific traffic situations, such as highly congested segments or complex merging and lane-changing behaviors, that were not fully captured during the calibration process. Furthermore, the higher relative variability in the error distribution, as reflected in the coefficient of variation, indicates that although the calibration enhanced average performance, its efficacy varied depending on traffic conditions. This variability may stem from the limitations of the selected model parameters, which might not fully account for certain driver behaviors unique to the selected highway segment. For example, local driving patterns, such as aggressive merging or braking, may not have been adequately represented in the calibration dataset. These findings highlight potential areas for future improvement, including incorporating additional behavioral data or refining the calibration parameters to better capture such specific scenarios.

To have a deeper comparison of the simulation results before and after the calibration process with the ground truth, the vehicle speed data collected by the RTMS are compared to the data collected from the simulations at data collection points. Although this comparison is not used for the optimization process, it provides valuable data about the calibration performance. The installed RTMS cover five different sections of the main highways and exits. Detailed information about these sections is presented in Table 4.

Table 4. The details of sections used to speed data collection.

Location ID	ID in the Simulation	Number of Lanes	Section Type
Location 1	Link 6	3	Main Road
Location 2	Link 7	1	Exit Ramp
Location 3	Link 29	2	Main Road
Location 4	Link 30	2	Exit Ramp
Location 5	Link 33	4	Main Road

Figure 7 compares the ground truth vehicle speed (RTMS) with vehicle speeds from the simulation both before and after the calibration process. The calibrated simulations showed improved alignment with the real-world measurement data, particularly displaying more stable speed patterns across main roads and exit ramps. This indicates that the calibration successfully refined the simulation parameters to mimic actual driving conditions better, thus enhancing the reliability of the traffic models for predictive analyses and planning decisions. However, as depicted in the figures, the vehicle speeds in the simulation network still generally exceed the ground truth speeds, even after calibration. Further examination of vehicle behavior in the calibrated simulation revealed that real-world drivers reduce their speed slightly in response to changes in road characteristics, such as entering a curve, an exit ramp, or encountering different road surfaces. Notably, two RTMS are located on an exit ramp and others near or before a curve. It can be concluded that the simulation did not adequately mimic this real-world speed reduction, warranting further investigation.

Figure 7. Average speed comparison of ground truth and simulation results before and after the calibration process.

4.2. Validation Results

Through multiple runs, the optimization process was able to determine the ideal calibration parameter values, greatly minimizing the differences between the simulation and the real world. To validate the calibrated parameter values across different traffic patterns and volumes, this study included a validation phase. The calibration was conducted using datasets collected during afternoon peak hours, from 1 PM to 4 PM. Validation was performed using separate datasets collected during morning peak hours, from 7 AM to 9 AM. The morning peak dataset was selected to test the model's robustness under different

traffic conditions. Morning traffic typically includes higher commuter volumes, different congestion patterns, and potentially more variable speeds compared to afternoon peak hours. This variation provides a challenging scenario to evaluate the model's generalizability and validate its performance across diverse traffic conditions. The VISSIM model was first run with the calibration parameters set to their default values, and the total error corresponding to these values was computed. Subsequently, the parameters were adjusted to the calibrated values, and the total error for these calibrated parameters was recorded. The differences between the default model and the calibrated model in the validation process are shown in Table 5.

Table 5. Statistical results of the errors in the validation process.

Errors in Time–Space Diagrams	Before Calibration	After Calibration	% of Change	Units
Mean	366.89	246.97	32.68%	m·min
Median	203.55	235.69	−15.79%	m·min
Standard Deviation	494.95	184.44	62.74%	m·min
Minimum	3.71	4.72	−27.23%	m·min
Maximum	2479.92	705.35	71.56%	m·min
25th percentile	23.39	85.17	−264.11%	m·min
75th percentile	558.05	375.83	32.65%	m·min
Variance	244,973.86	34,017.95	86.11%	(m·min)^2
Skewness	2.51	0.55	78.16%	-
Kurtosis	8.46	−0.40	104.69%	-
Coefficient of Variation	1.35	0.75	44.64%	-

In the validation phase, a significant reduction in mean error by 32.68% from 366.89 to 246.97 m·min was achieved, surpassing the improvement noted during calibration. This suggests that the calibrated parameters effectively enhanced the average accuracy of the model even under varying traffic conditions. However, the median error in the validation results increased by 15.79%, indicating that while some scenarios saw substantial improvements, typical cases represented by the median did not benefit uniformly. This tension between metrics indicates that while the calibration effectively addressed worst-case scenarios, it may have introduced trade-offs in handling typical or best-case scenarios. These findings highlight the potential need for future refinements to better balance improvements across the entire error distribution, ensuring consistent benefits for all traffic conditions. The reduction in the standard deviation during validation was profound, dropping by 62.74%, compared to a more modest 5.88% during calibration. This marked decrease underscores a significant enhancement in error consistency, suggesting that the variability in model performance was substantially narrowed after applying the calibrated parameters. The maximum error reduction during validation was also notable, decreasing by 71.56%, a substantial improvement that highlights the calibration's effectiveness in reducing worst-case scenario errors. Conversely, the minimum error and the 25th percentile error showed deteriorations, increasing by 27.23% and 264.11%, respectively. These results indicate that while extreme errors were better controlled, the best-case scenario performance worsened, and lower quartile errors became more prevalent. Skewness and kurtosis changes during validation showed a trend toward a more symmetric and flatter error distribution, contrasting with the increases observed during calibration. This suggests that while the calibration process helped reduce outliers, it also shifted the overall distribution of errors.

The validation results affirm the effectiveness of the calibration process in enhancing model accuracy and consistency across different testing conditions. However, the increase in median and 25th percentile errors alongside the variability in skewness and kurtosis across different datasets point to areas where further calibration refinement could be beneficial. This highlights the importance of tailoring calibration strategies to accommodate variations in traffic patterns and conditions to ensure the model's robustness and reliability.

Data gathered from the simulations and RTMS are used to compare the average vehicle speed before and after the calibration of parameters with the ground truth data. The validation process's average speed data from 7 to 9 AM are displayed in Figure 8. Although they still require improvement, the calibrated parameters considerably decreased the differences between the simulation and the ground truth, as shown in the figure.

Figure 8. Average speed comparison of ground truth and simulation results before and after implementing calibrated parameters in the validation process.

These calibrated traffic simulation models have significant practical applications in traffic engineering. For instance, the improved model accuracy can support enhanced ramp metering strategies, where precise predictions of traffic flows are essential to managing merging and lane-changing scenarios effectively. Similarly, the reduced error variability allows for better corridor management, enabling traffic engineers to design adaptive signal timings and manage traffic congestion dynamically. These applications demonstrate how the proposed calibration framework can translate into actionable insights for real-world traffic management and planning tasks.

5. Discussion and Conclusions

This study effectively illustrated how a VISSIM microsimulation model can be calibrated and its ability to simulate a real-world highway segment (a section of the NJ-3 and NJ-495 eastbound highways in Hudson County, New Jersey) improved by using connected vehicle data from the Wejo dataset. Our goal was to apply a GA to connected vehicle data from the Wejo dataset in order to decrease trajectory inconsistencies in a VISSIM microsimulation model. The objective of this work was to increase simulation accuracy and model fidelity by utilizing high-resolution trajectory data and iterative optimization.

The study's findings, which show notable error reductions across important measures, highlight the value of combining GAs for calibration with connected vehicle trajectory data. This study emphasizes the benefits of VISSIM's compliance with high-resolution trajectory data and distributed computing architecture when comparing the findings to other research, such as Leal et al. [8], which also used GAs but concentrated on AIMSUN software (version not specified). Likewise, the strategy employed here provides more scalability and flexibility for a variety of traffic networks than approaches such as multi-point distribution calibration [29] or Bayesian neural networks [13]. This approach can be used to increase simulation fidelity in both urban and highway settings, as evidenced by the observed improvement in trajectory alignment, especially in the mean and median error reductions. The accuracy of the model was significantly improved by this calibration, as shown by the drop in mean and median errors as well as a general decrease in the variability of error metrics after calibration. The mean error decreased by 14.19%, while the median error saw an 18.27% reduction, showcasing the effectiveness of the calibration process in improving overall accuracy.

The results underscore the importance of accurate parameter tuning in traffic simulation models and illustrate the benefit of leveraging connected vehicle data. By offering a unique calibration framework that goes beyond conventional techniques that rely on fixed parameter values or limited data sources, this study advances the discipline. This technique presents a dynamic and data-driven solution that may adjust to the particular features of any traffic network by utilizing connected vehicle trajectory data. By making traffic simulation models more realistic and applicable, this invention makes it possible to analyze and prepare for contemporary transportation systems with greater accuracy. Particularly notable was the rapid convergence to optimal parameter values within the first quarter of the iterations, highlighting the efficiency of the GA in finding practical solutions quickly. However, increased skewness and kurtosis post-calibration suggest that while the average errors were reduced, the variability, in some cases, increased. The increases in skewness and kurtosis indicate that while the overall error is reduced, certain extreme cases still exist, which could point to specific traffic behaviors not fully captured by the calibration. This suggests potential areas for further refinement, such as incorporating more detailed behavioral models or data sources.

The suggested strategy has a few limitations despite its proven efficacy. First, even though the GA effectively reduced the number of discrepancies in this investigation,

other optimization methods or hybrid approaches might produce even better outcomes. Furthermore, the framework does not yet take into consideration extremely specific driving behaviors or external variables that could affect calibration results, such as weather or incident impacts. By extending the calibration to multi-network settings, adding more data sources, and investigating sophisticated optimization strategies, future work will overcome these constraints. The calibration procedure might also be improved by using a multi-criteria objective function or a more complicated objective function.

The calibrated models have significant practical implications for traffic engineering, such as improving ramp metering strategies, optimizing corridor management, and aiding in the development of adaptive traffic signal systems. By providing more realistic simulations, the approach enables traffic engineers and planners to make better-informed decisions for infrastructure design and operational strategies. The approach outlined in this paper not only provides a robust framework for enhancing the fidelity of traffic simulations but also offers a scalable method that can be applied to other segments or networks, irrespective of their specific characteristics or geographic locations. As cities and transportation networks continue to evolve, the integration of advanced simulation tools with real-world data will be crucial in designing more efficient and sustainable traffic systems.

Author Contributions: Conceptualization, J.L., B.D. and L.S.; methodology, J.L., A.A. and D.B.; software, J.L. and A.A.; validation, J.L. and A.A.; formal analysis, A.A. and J.L.; resources, D.B.; writing—original draft preparation, A.A.; writing—review and editing, J.L. and B.D.; visualization, A.A.; supervision, J.L. and L.S.; project administration, D.B.; funding acquisition, D.B. and L.S. All authors have read and agreed to the published version of the manuscript.

Institutional Review Board Statement: Not applicable.

Informed Consent Statement: Not applicable.

Data Availability Statement: The data used in this study are available from the corresponding author upon reasonable request.

Conflicts of Interest: The authors declare no conflicts of interest. The funders had no role in the design of the study; in the collection, analyses, or interpretation of data; in the writing of the manuscript; or in the decision to publish the results.

References

1. Alghamdi, T.; Mostafi, S.; Abdelkader, G.; Elgazzar, K. A Comparative Study on Traffic Modeling Techniques for Predicting and Simulating Traffic Behavior. *Future Internet* **2022**, *14*, 294. [CrossRef]
2. Arora, N.; Chen, Y.; Ganapathy, S.; Li, Y.; Lin, Z.; Osorio, C.; Tomkins, A.; Tsogsuren, I. An Efficient Simulation-Based Travel Demand Calibration Algorithm for Large-Scale Metropolitan Traffic Models. *arXiv* **2021**, arXiv:2109.11392. [CrossRef]
3. Tang, L.; Zhang, D.; Han, Y.; Fu, A.; Zhang, H.; Tian, Y.; Yue, L.; Wang, D.; Sun, J. Parallel-Computing-Based Calibration for Microscopic Traffic Simulation Model. *Transp. Res. Rec. J. Transp. Res. Board* **2024**, *2678*, 279–294. [CrossRef]
4. Keane, R.; Gao, H.O. Fast Calibration of Car-Following Models to Trajectory Data Using the Adjoint Method. *Transp. Sci.* **2021**, *55*, 592–615. [CrossRef]
5. Tang, Y.; Jin, L.; Ozbay, K. Physics-Informed Machine Learning for Calibrating Macroscopic Traffic Flow Models. *arXiv* **2023**, arXiv:2307.06267. [CrossRef]
6. Anil Chaudhari, A.; Srinivasan, K.K.; Rama Chilukuri, B.; Treiber, M.; Okhrin, O. Calibrating Wiedemann-99 Model Parameters to Trajectory Data of Mixed Vehicular Traffic. *Transp. Res. Rec.* **2022**, *2676*, 718–735. [CrossRef]
7. Khaleghian, S.; Neema, H.; Sartipi, M.; Tran, T.; Sen, R.; Dubey, A. Calibrating Real-World City Traffic Simulation Model Using Vehicle Speed Data. In Proceedings of the 2023 IEEE International Conference on Smart Computing (SMARTCOMP), Nashville, TN, USA, 26–30 June 2023; pp. 303–308.

8. Leal, S.S.; Maciel De Almeida, P.E.; Ribeiro, R.G. Calibrating Traffic Microscopic Simulation Model Parameters Using an Evolutionary Approach. *Transp. Res. Procedia* **2020**, *48*, 1038–1045. [CrossRef]

9. Arafat, M.; Nafis, S.R.; Sadeghvaziri, E.; Tousif, F. A Data-Driven Approach to Calibrate Microsimulation Models Based on the Degree of Saturation at Signalized Intersections. *Transp. Res. Interdiscip. Perspect.* **2020**, *8*, 100231. [CrossRef]

10. Englezou, Y.; Timotheou, S.; Panayiotou, C.G. A Probabilistic Approach for the Calibration of Incomplete Microscopic Traffic Models. In Proceedings of the 2023 IEEE 26th International Conference on Intelligent Transportation Systems (ITSC), Bilbao, Spain, 24–28 September 2023; pp. 4266–4271.

11. Rutter, C.M.; Ozik, J.; DeYoreo, M.; Collier, N. Microsimulation Model Calibration Using Incremental Mixture Approximate Bayesian Computation. *Ann. Appl. Stat.* **2019**, *13*, 2189. [CrossRef] [PubMed]

12. Wade, S.; Weber, M.F.; Sarich, P.; Vaneckova, P.; Behar-Harpaz, S.; Ngo, P.J.; Cressman, S.; Gartner, C.E.; Murray, J.M.; Blakely, T.A.; et al. Bayesian Calibration of Simulation Models: A Tutorial and an Australian Smoking Behaviour Model. *arXiv* **2022**, arXiv:2202.02923. [CrossRef]

13. Chen, Q.; Ni, A.; Zhang, C.; Wang, J.; Xiao, G.; Yu, C. A Bayesian Neural Network-Based Method to Calibrate Microscopic Traffic Simulators. *J. Adv. Transp.* **2021**, *2021*, 4486149. [CrossRef]

14. Naing, H.; Cai, W.; Wu, T.; Yu, L. Dynamic Car-Following Model Calibration with Deep Reinforcement Learning. In Proceedings of the 2022 IEEE 25th International Conference on Intelligent Transportation Systems (ITSC), Macau, China, 8–12 October 2022; pp. 959–966.

15. Hwang, J.; Ko, S.; Au, T.-C. Calibrating Dynamic Traffic Assignment Models by Parallel Search Using Active-CMA-ES. In Proceedings of the 2021 IEEE International Intelligent Transportation Systems Conference (ITSC), Indianapolis, IN, USA, 19–22 September 2021; pp. 3265–3270.

16. Abdelhalim, A.; Abbas, M.; Kotha, B.B.; Wicks, A. A Framework for Real-Time Traffic Trajectory Tracking, Speed Estimation, and Driver Behavior Calibration at Urban Intersections Using Virtual Traffic Lanes. In Proceedings of the 2021 IEEE International Intelligent Transportation Systems Conference (ITSC), Indianapolis, IN, USA, 19–22 September 2021; pp. 2863–2868.

17. Langer, M.; Harth, M.; Preitschaft, L.; Kates, R.; Bogenberger, K. Calibration and Assessment of Urban Microscopic Traffic Simulation as an Environment for Testing of Automated Driving. In Proceedings of the 2021 IEEE International Intelligent Transportation Systems Conference (ITSC), Indianapolis, IN, USA, 19–22 September 2021; pp. 3210–3216.

18. Shoaib Samandar, M.; Chun, G.; Yang, G.; Chase, T.; Rouphail, N.M.; List, G.F. Capitalizing on Drone Videos to Calibrate Simulation Models for Signalized Intersections and Roundabouts. *Transp. Res. Rec. J. Transp. Res. Board* **2022**, *2676*, 96–111. [CrossRef]

19. Hale, D.K.; Ghiasi, A.; Khalighi, F.; Zhao, D.; Li, X.; James, R.M. Vehicle Trajectory-Based Calibration Procedure for Microsimulation. *Transp. Res. Rec. J. Transp. Res. Board* **2023**, *2677*, 1764–1781. [CrossRef]

20. Kaths, H.; Keler, A.; Bogenberger, K. Calibrating the Wiedemann 99 Car-Following Model for Bicycle Traffic. *Sustainability* **2021**, *13*, 3487. [CrossRef]

21. Haque, M.S.; Zhao, L.; Rilett, L.R.; Tufuor, E.O.A. Calibration and Validation of a Microsimulation Model of Lane Closures on a Two-Lane Highway Work Zone. *Transp. Res. Rec. J. Transp. Res. Board* **2023**, *2677*, 974–990. [CrossRef]

22. Zhao, L.; Rilett, L.R.; Shakiul Haque, M. Calibration and Validation Methodology for Simulation Models of Intelligent Work Zones. *Transp. Res. Rec.* **2022**, *2676*, 500–513. [CrossRef]

23. Chun, G.; Rouphail, N.; Samandar, M.S.; List, G.; Yang, G.; Akçelik, R. Analytical and Microsimulation Model Calibration and Validation: Application to Roundabouts under Sight-Restricted Conditions. *Transp. Res. Rec. J. Transp. Res. Board* **2023**, *2677*, 274–288. [CrossRef]

24. Abdeen, M.A.R.; Farrag, S.; Benaida, M.; Sheltami, T.; El-Hansali, Y. VISSIM Calibration and Validation of Urban Traffic: A Case Study Al-Madinah City. *Pers. Ubiquitous Comput.* **2023**, *27*, 1747–1756. [CrossRef]

25. Bowman, C.; Miller, J.A.; Wang, Y. Microscopic Vehicular Traffic Simulation: Comparison of Calibration Techniques. In Proceedings of the 2022 Winter Simulation Conference (WSC), Singapore, 11–14 December 2022; pp. 2234–2245.

26. Figueiredo, M.; Seco, Á.; Silva, A.B. Calibration of Microsimulation Models—The Effect of Calibration Parameters Errors in the Models' Performance. *Transp. Res. Procedia* **2014**, *3*, 962–971. [CrossRef]

27. Ištoka Otković, I.; Tollazzi, T.; Šraml, M. Calibration of Microsimulation Traffic Model Using Neural Network Approach. *Expert Syst. Appl.* **2013**, *40*, 5965–5974. [CrossRef]

28. Mauro, R.; Giuffrè, O.; Granà, A.; Chiappone, S. A Statistical Approach for Calibrating a Microsimulation Model for Freeways. *WSEAS Trans. Environ. Dev.* **2014**, *10*, 496–508.

29. Gao, Y.; Zhou, C.; Rong, J.; Zhang, X.; Wang, Y. Enhancing Parameter Calibration for Micro-Simulation Models: Investigating Improvement Methods. *Simul. Model. Pract. Theory* **2024**, *134*, 102950. [CrossRef]

30. Tousi, S.M.A.; Samizadeh, S.; Nikoofard, A. Genetic Algorithm in Traffic Control and Autonomous Driving. In *Frontiers in Genetics Algorithm Theory and Applications*; Khosravy, M., Gupta, N., Witkowski, O., Eds.; Springer Tracts in Nature-Inspired Computing; Springer Nature: Singapore, 2024; pp. 195–208. ISBN 978-981-9981-06-9.

31.   Alkafaween, E.; Hassanat, A.; Essa, E.; Elmougy, S. An Efficiency Boost for Genetic Algorithms: Initializing the GA with the Iterative Approximate Method for Optimizing the Traveling Salesman Problem—Experimental Insights. *Appl. Sci.* **2024**, *14*, 3151. [CrossRef]

32.   Hassanat, A.; Almohammadi, K.; Alkafaween, E.; Abunawas, E.; Hammouri, A.; Prasath, V.B.S. Choosing Mutation and Crossover Ratios for Genetic Algorithms—A Review with a New Dynamic Approach. *Information* **2019**, *10*, 390. [CrossRef]